Intra–inter polyad mixing and breaking of symmetric–antisymmetric selection rule in the vibrational spectra of CS_2 molecule

J. P. Pique[a)]
Laboratoire de Spectrométrie Physique,[b)] Université Joseph Fourier de Grenoble, B.P. 87, 38402 Saint Martin d'Hères Cedex, France

J. Manners
The Open University, Physics Department, Walton Hall, Milton Keynes, MK7 6AA United Kingdom

G. Sitja and M. Joyeux
Laboratoire de Spectrométrie Physique,[b)] Université Joseph Fourier de Grenoble, B.P. 87, 38402 Saint Martin d'Hères Cedex, France

(Received 1 May 1991; accepted 22 January 1992)

A laser system composed of tunable lasers pumped by a copper vapor laser (Oxford Lasers Cu60) is described in this paper. The high resolution obtained with this system has allowed excitation of selective rotational levels of the 15 V and 10 V vibrational bands of the $V\,^1B_2$ excited electronic state of the CS_2 molecule in its vapor phase ($\sim$100 mTorr). The rotational assignment of the excitation spectra was accomplished by observing the dispersed fluorescence. We show that it is not necessary to use a supersonic jet in order to assign the emission spectra of CS_2. The goal of this work is to study the highly excited vibrational states of the ground electronic state of CS_2 up to the first dissociation limit. For our purpose, there are two important consequences of the particular geometry of the 15 V excitation, which is just below and close to the bending potential barrier of the $V\,^1B_2$ state. First, a very good Franck–Condon overlap in the excitation and a large Franck–Condon access to high vibrational states, as high as 20 000 cm^{-1}, allow observation of the dispersed fluorescence through a high resolution monochromator with an OMA detector. This avoids the need for more complicated techniques, like SEP spectroscopy. Moreover, we show for the first time, that, in the $V\,^1B_2$ excited state, a strong Coriolis interaction $Q_2^3\,Q_3\,J_c$ couples the bending (0,3,0) and antisymmetric stretching levels (0,0,1). This breaking of the symmetric–antisymmetric selection rule gives access to the antisymetric stretching levels of the ground electronic state $\tilde{X}\,\Sigma_g^+$ from the 15 V excitation. We also show that, below 12 000 cm^{-1}, the vibrational couplings of CS_2 can be described by a model of 2 degrees of freedom, which includes a strong 1:2 Fermi resonance and accidental resonant perturbations between adjacent polyads which is probably a first step in the transition to a chaotic regime in CS_2.

I. INTRODUCTION

From the point of view of the study of quantum chaos the CS_2 molecule presents several advantages, both from the experimental and the theoretical standpoint. These are the following: (i) Mulliken[1] has suggested that the lowest electronic states of CS_2 should be analogous to those of the CO_2 molecule, which has already been extensively theoretically studied (CO_2 and CS_2 have the same number of valence electrons); (ii) the absorption of CS_2 is in the near uv with a maximum at about 320 nm, which allows easier excitation than CO_2 (210 nm); (iii) its fluorescence spectrum extends far into the red on account of the large difference in geometry between the ground and excited electronic states; (iv) it is triatomic, which is the minimum atomicity for which we can hope to observe vibrational chaos and the maximum atomicity if we wish to perform precise, semiclassical and *ab initio* calculations; (v) the experimental and theoretical study of purely vibrational chaos in the ground electronic state, Σ_g^+, is possible since the first observed excited state is above 26 000 cm^{-1} (Ref. 2); (vi) CS_2 spectra reveal strong Fermi resonances; consequently, as it has been shown in several theoretical works, strong resonances usually lead to mode mixing which could induce a chaotic situation.

The first studies of the absorption spectra of gaseous CS_2 between 290 and 430 nm (Refs. 2 and 3) have shown the existence of two principal bands called R (330–430 nm) and V (290–330 nm), the second being very much more intense than the first. The observation of a magnetic rotation spectrum[4] and of a weak magnetic moment detected using the Hanle effect,[5] (in spite of the absence of the Zeeman effect[6]), shows that V is a singlet state coupled with a state of nonzero spin. Jungen *et al.*[3] attributes this to the bent $^1B_2$ state, correlated with the $^1\Delta_u$ state of the linear molecule. The R state is the spin component B_2 of the state $^3A_2$ correlated with a $^3\Delta_u$ state of the linear molecule.[6,7] The study of the influence of rotation and vibration on the lifetimes of the excited electronic states shows that R and V are coupled by a strong spin–orbit interaction.[8] Similarly, the V state seems

[a)] To whom correspondence should be addressed.
[b)] Associated to C. N. R. S. URA 08.

 0021-9606/92/096495-14$06.00

to be coupled by a spin–rotation interaction with the spin component A_1 and B_1 of the $^3A_2$ triplet state.[9] The $G(0,0,0)$ level of the R state seems to be situated at 26 187 cm^{-1} (Ref. 2); the energy of the $G(0,0,0)$ level of the V state remains in doubt since Jungen *et al.*[3] puts it at 30 904 cm^{-1}, Kasahara *et al.*[10] at 30 542 cm^{-1}, and Ochi *et al.*[9] in the region of 30 200 cm^{-1}.

The dispersed fluorescence spectra of CS_2 allow access to the highly excited vibrational states of the $\tilde{X}\,\Sigma_g^+$ state. However, these spectra have been studied to a far lesser extent than the absorption spectra: Silvers *et al.*[11] and Matsuzaki *et al.*[12] were the first to report such spectra, excited by a nitrogen laser. They did not observe levels beyond a vibrational energy of 4500 cm^{-1}. Bernath *et al.*[13] and Vasudev[14] used, respectively, argon or krypton ion lasers and a tripled Nd:YAG to excite the R state of CS_2. Bernath reports around 40 levels between 0 and 12 000 cm^{-1} and Vasudev about 90 levels up to a vibrational energy of 12 000 cm^{-1}. Apart from Matsusaki *et al.*[15] whose spectra had a resolution of 10 Å, only Kasahara *et al.*[10] has excited CS_2 in the V state, in which the absorption is an order of magnitude greater than in the R state, and this was achieved using a dye-laser pumped by a nitrogen or Nd:YAG laser. They report around 80 levels up to 13 000 cm^{-1}. Unfortunately, the spectral widths both of their laser (1 cm^{-1}) and their spectrometer (10 cm^{-1}) are not sufficient to allow them to excite and observed a unique rovibronic level. The common point of all of these studies is that only those levels without antisymmetric stretching and of a given parity of bending vibration have been observed.

Bernath *et al.*[13] and Vasudev[14] have used the levels that they have observed to fit an effective Hamiltonian involving about 12 parameters deduced from the ir data.[16,17] Vasudev does not give the uncertainties in the parameters, and the uncertainties in the parameters given by Bernath *et al.* are anormally small compared with the differences between the observed and calculated frequencies (sometimes greater than 4 cm^{-1}). It is therefore impossible to discern which parameters of the Hamiltonian are significant.

From the literature which we have outlined above, it became apparent to us that the published results were not sufficient to be used as a basis for a serious attempt at modeling the CS_2 molecule. We therefore embarked upon a study of the emission spectrum from the $V\,^1B_2$ state to the $\tilde{X}\,\Sigma_g^+$ state, paying particular attention to the following points: (i) will the excitation of a single rovibronic level of a strong transition in the V absorption band, coupled with sensitive and high resolution detection, allow us to observe a density of levels significantly greater than those reported so far (ii) since the 1:2 resonance between the symmetric stretching and the bending modes strongly couples all of the levels in a polyad, how does one describe the levels observed in the spectra other than by the quantum numbers v_1 and v_2 which are no longer good quantum numbers? (iii) Up to what energy can the CS_2 molecule be considered to be a molecule of 2 degrees of freedom, or is it that the absence of levels with $v_3 > 0$ (antisymmetric stretching) in previous experiments is ascribable to inadequate resolution or signal to noise ratio? (iv) Which of the parameters in the effective Hamiltonian are significant for a description of the highly excited vibrational states in CS_2?

In this paper we report low resolution (3 cm^{-1}) spectra of the vibrational levels of the $\tilde{X}\,\Sigma_g^+$ ground electronic state up to 18 000 cm^{-1}. We discuss in detail the first part up to 12 000 cm^{-1}. The second part will be discussed in a forthcoming paper through high resolution spectra.

The plan of this publication is as follows: in the first part we describe our Cu vapor laser system and discuss the various ways in which we can access the high vibrational energies of the $\tilde{X}\,\Sigma_g^+$ ground state of the CS_2 molecule. We then show, by comparison with the absorption spectra obtained by Ochi *et al.*[9] using a supersonic jet, that it is possible to excite a single rotational line of the 15 V and 10 V bands in the vapor phase and we identify the transitions using the dispersed fluorescence spectra. We discuss and fit an effective Hamiltonian on the basis of our dispersed fluorescence results. In the light of this fit, we show that strong vibrational perturbations, in addition to the 1:2 Fermi resonance, appear in the ground electronic state. We also show that intense transitions to the antisymmetric stretching mode appear in the dispersed fluorescence spectra, when the molecule is excited in the 15 V band (31 346 cm^{-1}). Finally, we discuss these observations in terms of inter polyad resonances in the ground state and a strong Coriolis coupling in the 15 V band of the excited state.[18]

This paper gives the experimental information used in Refs. 19 and 20 which analyze the dynamics of CS_2 both through statistical methods and in the phase space, which topology is determined at the semiclassical limit, using the molecular constants which fit the experimental spectra.

II. THE COPPER VAPOR LASER SYSTEM

The experimental arrangement is shown in Fig. 1. Our laser system is based around a 60 W Oxford Lasers copper vapor laser. The high efficiency of this laser and its emission in the visible region of the spectrum (511 and 578 nm) have motivated many countries to employ it in uranium isotope separation. One would therefore assume that its reliability can only improve. Before the advent of this laser, lasers used in spectroscopy fell into two broad categories: pulsed lasers such as YAG or excimer, or continuous wave lasers such as argon or krypton ion. These latter lasers did not allow easy production of powerful and tunable uv beams. In general, pulsed lasers have a relatively low repetition rate (< 100 Hz) but high peak powers can be obtained from a tunable laser pumped by these lasers. Thus frequency doubling is easily achieved, but it is also easy to saturate the transitions of the molecules under study and to avoid undesirable multiphoton effects it is often necessary to attenuate the laser intensity. It therefore becomes preferable to spread the energy over time. The high repetition rate of the copper vapor laser (5 to 30 kHz) with its, nevertheless, reasonably high peak power (250 kW for a mean power of 50 W, a repetition rate of 6.5 kHz, and a pulse duration of 50 ns) make it, in our view, a useful instrument for spectroscopy. The poor spatial quality of the beam in the plane–plane cavity (spatial fluctu-

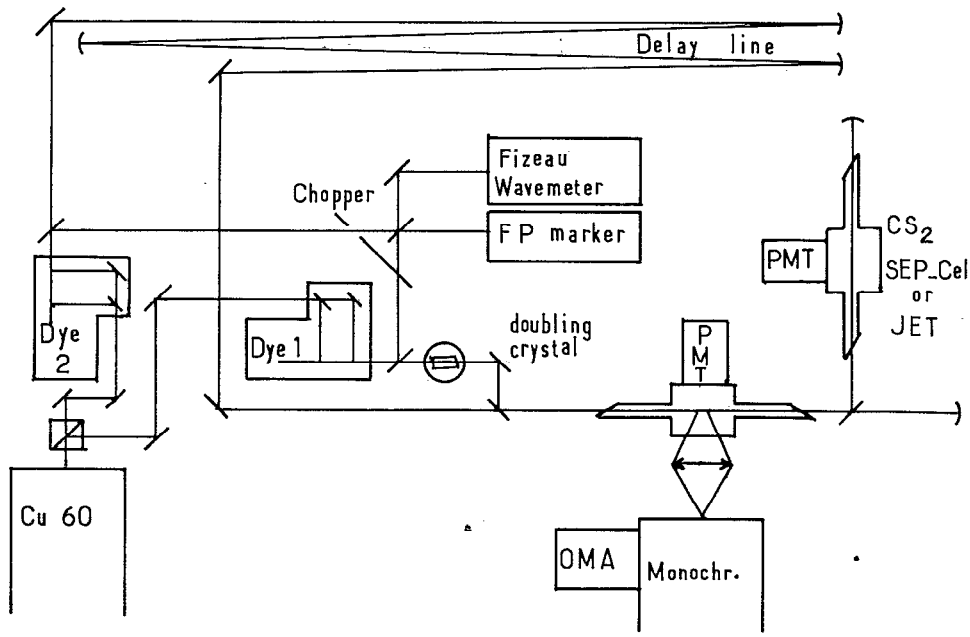

FIG. 1. The copper vapor laser setup.

ations in the intensity and divergence) has led us to adopt an unstable cavity mounted directly on the optical table. It has been necessary to suppress air currents in the laser cavity which cause instabilities. Since it was not possible to find a commercial dye laser that could be optimized to be pumped by the copper vapor laser, we have constructed two types of laser: two dye lasers and a titanium–sapphire laser. The dye lasers each consist of an oscillator and one or two amplifiers. The oscillator is composed of a special grazing incidence grating (Jobin Yvon) and a beam expander consisting of two prisms. A new design of dye cell had to be developed in order to obtain a sufficiently high dye flow speed to ensure renewal of the dye between each pulse. The resultant spectral width is in the best conditions 0.02 cm^{-1}. Figure 2(c) shows the linewidth of the laser by means of a SEP (simulated emission pumping) spectrum of CS_2. Tuning is achieved by rotating a mirror. This rotation has a precision of 1/10 000 deg, which is compatible with the laser linewidth. The movement of the rotating mirror allows linear tuning of the wavelength by the use of a deformable triangle operating near the elastic limit of the material of the triangle. This method avoids tuning irregularities caused by friction between two mechanical items. The efficiency of the dye lasers depends both on the dye used and on the resolution required (which can be easily adjusted). Typically, it is of the order of 15% for a resolution of 2 GHz. An ADP* crystal mounted directly in front of the output of the last amplifier allows frequency doubling with an efficiency of the order of 7%. The use of a BBO crystal has allowed us to obtain a uv output of the order of 0.5 W.

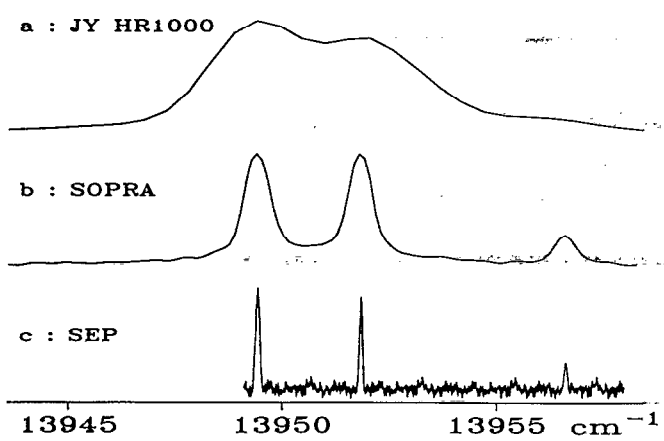

FIG. 2. Example of an emission spectrum arising from the $R(4)$ rotational line of the 15 V band, using: (a) the Jobin Yvon HR1000 monochromator, (b) the SOPRA monochromator, and (c) the SEP technique. The linewidth of the last spectrum is 0.04 cm^{-1}; this corresponds to a dye laser linewidth of 0.02 cm^{-1} at 640 nm.

The peak power of the copper vapor laser is sufficient to give efficient frequency doubling, but, nevertheless, remains within the range suitable for pumping a titanium–sapphire crystal in a cavity of the type usually used for continuous wave operation, which we have specifically developed[21,22] for use with the copper vapor laser. The dynamics of this system is quite remarkable. Efficiencies of 20% have been obtained. The two copper vapor laser beams at 511 and 578 nm efficiently pump the titanium–sapphire laser which can operate between 680 and 1100 nm. Extension of the wavelength range of the laser to between 340 and 550 nm can easily be achieved by frequency doubling.

Many experimental methods have been employed in order to study the high vibrational energies of the ground electronic state of CS_2: dispersed fluorescence (DF), stimulated emission pumping (SEP), intracavity SEP, stimulated photon echoes (SPE), and Fourier transform spectroscopy

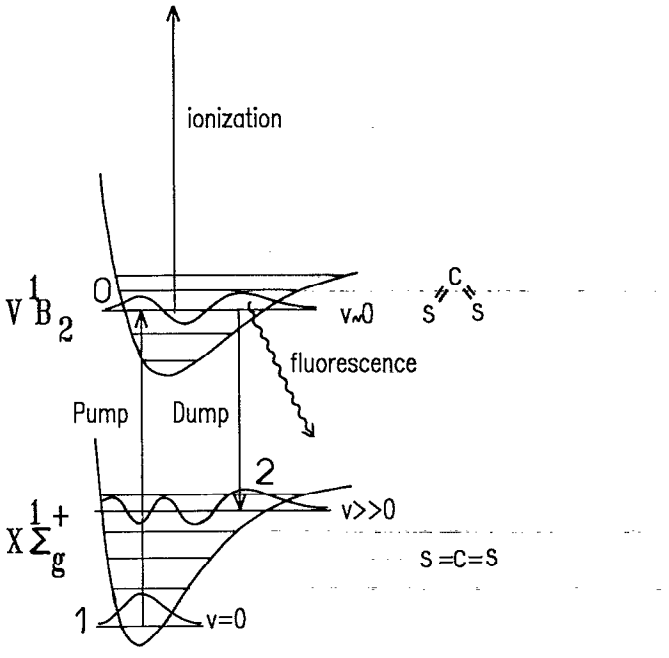

FIG. 3. Experimental methods. See the text.

(FTS). The initial stage of all of these methods is to use one laser (the pump) to prepare an initial state in the $V\,{}^1B_2$ state of CS_2 (Fig. 3). The first method consists of dispersing the spontaneous fluorescence in a monochromator equipped with an OMA. The difference in geometry between the $\tilde{X}\,\Sigma_g^+$ ground state and the excited $V\,{}^1B_2$ state results in a maximum in the Franck–Condon factor in the red (see later) and allows it to reach 18 000 cm^{-1} above the ground state. This energy corresponds to about 40 vibrational quanta in the bending mode. Beyond that it is necessary to use the SEP technique. In this case a second laser is brought into resonance with an $\tilde{X}\,\Sigma_g^+ \rightarrow V\,{}^1B_2$ transition, and the SEP spectrum can be obtained by various detection methods: reduction in the fluorescence intensity,[23] polarization modification, and ionization.[24] The sensitivity of SEP can be increased by at least 2 orders of magnitude by an intracavity method.[21,25] The SPE technique consists of producing a photon echo on a black background after a series of three pulses (pump–dump–pump) suitably polarized and phased matched.[26] This technique has not allowed spectra to be easily obtained. FTS spectroscopy (with a BOMEM spectrometer) has also failed to produce satisfactory results. The photon noise due to a continuous fluorescent background from CS_2 seriously limits the FTS technique for this molecule.

The majority of the results presented in this paper were obtained using the DF technique. The 15 V (31 346.45 cm^{-1}) and 10 V (30 899.29 cm^{-1}) vibrational bands were chosen for the initial excitation. A mixture of the dyes DCM and R640 in methanol produces a mean power of several watts at 640 nm. The 511 and 578 nm beams from the Cu laser pump DCM and R640, respectively. The spectral density in the 15 V and 10 V bands is such that a resolution of 2 GHz is required in order to excite a single rotational level with the pump laser. The wavelength of this laser is measured using a Fizeau interferometer (Laser Technic) which gives an absolute precision of 1 GHz and a relative precision of 100 MHz.

For the excitation spectra (Fig. 1) we excite the molecule with radiation from the dye laser, and the total fluorescence is observed at 90° to the excitation using a photomultiplier (Hamamatsu R928) from which the output signal is taken to a boxcar averager (SRS SR250/SR280). A microcomputer IBM PC/XT collects the data from the Fizeau interferometer and the boxcar. For the resolved fluorescence spectra, the fluorescence traveling along the axis is reflected from a mirror which contains a hole through which the excitation beam passes. The fluorescence is then focused onto the entrance slit of a monochromator (Jobin Yvon HR1000 or SOPRA). The dispersed light then impinges on an array of photodiodes with an image intensifier (Princeton Instruments IRY-700G). The dispersions of the two monochromators are 0.18 and 0.02 Å/diode, respectively.

III. ROTATIONAL ASSIGNMENT OF THE 15 V ABSORPTION BAND OF THE VAPOR PHASE CS_2

The excitation spectrum of CS_2 at a pressure of 150 mTorr has been recorded between 31 338 and 31 348 cm^{-1} (Fig. 4) and between 30 896 and 30 906 cm^{-1} (Fig. 5). These bands, referred to by Jungen *et al.*[3] as 15 V and 10 V, are the most intense of the excitation spectrum between 2900 and 3600 Å. Furthermore, these bands do not overlap with the hot bands (Fig. 1 of Ref. 3). They correspond to the electronic transition $\tilde{X}\,\Sigma_g^+ \rightarrow V\,{}^1B_2$ where the state $V\,{}^1B_2$ is correlated with the higher energy Renner–Teller component of the $\pi \rightarrow \pi^*\,{}^1\Delta_u$ state of the linear molecule. Jungen *et al.*[3] have already assigned the rotational levels of the 10 V. As the 10 V and 15 V excitation bands have a particular importance in our work, we assigned the rotational levels of the 15 V band at room temperature.

Because the 15 V and 10 V bands are severely perturbed,[3] their excitation spectra are extremely congested, to such an extent that, some authors have preferred to use a

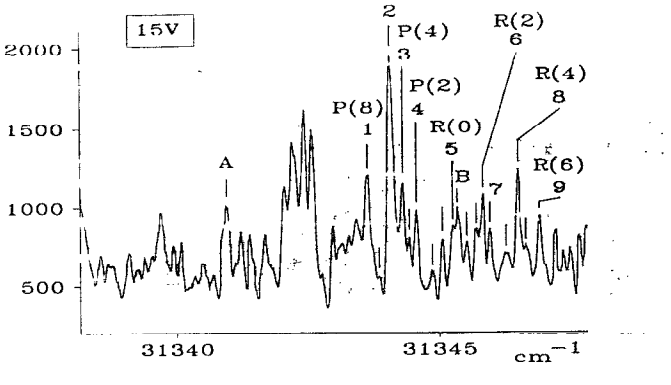

FIG. 4. Excitation spectrum of CS_2 band 15 V ($P = 150$ mTorr). Frequencies of lines marked with a dash are given in Table II. The numbers 1 to 9 refer to lines reported by Ochi *et al.* (Ref. 9) in their supersonic jet spectra.

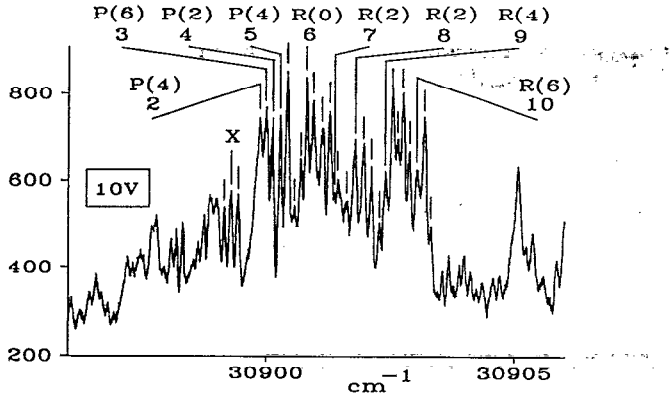

FIG. 5. Excitation spectrum of CS_2 band 10 V ($P = 150$ mTorr). The frequencies of lines marked with a dash are given in Table III. The numbers 2 to 10 refer to lines reported by Ochi *et al.* (Ref. 9) in their supersonic jet spectra.

supersonic jet. It is possible, however, to excite a single rotational level with a sufficiently narrow bandwidth laser (0.02 cm^{-1}). The experiments are thereby greatly simplified. In the vapor phase the spectra are a superposition of a quasicontinuum and a line structure. The origin of the continuous background has been discussed at length but is still not well understood. The dispersed fluorescence and the high resolution SEP spectra (Fig. 2) show that, even with a resolution of 2 GHz the continuous background is not resolved. The continuum was observed by Matsuzaki *et al.*[15] in the vapor phase at ambient temperature but not by Kasahara *et al.*[10] in a supersonic jet. Matsuzaki *et al.* suggest that the continuous background is the origin of the long lifetime component of the fluorescence. Kasahara *et al.*[10] favor the hypothesis of spectral congestion of several hot bands. This hypothesis does not seem to be supported by our results. We can, however, be certain that the continuous background cannot be attributed to a predissociating state since the excitation frequency ($\sim$31 200 cm^{-1}) is below the first dissociation limit of the $\tilde{X}\,\Sigma_g^+$ state, which is estimated to be at 35 970 $\pm$ 130 cm^{-1}. The linearity of the fluorescence with laser intensity also suggests that it is not due to multiphoton effects.

The existence of the continuous background does not prevent the excitation of a single rovibrational state of $V\,^1B_2$ or the study of the emission spectrum of the $\tilde{X}\,\Sigma_g^+$ ground state as long as a sufficiently narrow bandwidth laser is employed and a low CS_2 pressure is used. All our experiments were done at a pressure around 50 mTorr for which the collisions are negligible.[27] At this pressure the continuous background intensity is less than 1%.

The narrowest excitation lines observed in our spectra have a full width at half-maximum of 0.06 cm^{-1}, which is approximately equal to the Doppler width of the transition (0.05 cm^{-1}). Until now the 15 V band had not been assigned in the vapor phase. We have analyzed the rotational structure of the 15 V band by recording two dispersed fluorescence spectra of CS_2 at 600 and 680 nm. Having accomplished this we are then able to ensure that we excite a single rotational level. The most intense and most isolated transitions in the spectrum are labeled by A,1,2,B,6,8, and 9 on Fig. 4. The size of the gaps between the P–R doublets in the fluorescence lines at different wavelengths enables us to assign the transitions $P(8)$,$R(2)$,$R(4)$, and $R(6)$ to the lines 1,6,8, and 9 and $P(16)$ or $P(18)$ to the line A (cf. Table I). All of the results for the 15 V band are shown in Table II together with the values published by Ochi *et al.*[9] for the spectra obtained using a supersonic jet. Our assignments are identical with Ochi's and the frequencies agree to within about 1 GHz. The intensities are, of course, different on account of the low rotational (< 10 K) and vibrational (220 K) temperatures in the supersonic jet. A high resolution experiment has shown us that lines 2 and B are a superposition, respectively, of lines $P(6)$ and $R(0)$ with hot band lines.

The lines in band 10 V have been assigned by comparison with the spectra of Jungen *et al.*[3] and Ochi *et al.*,[9] the

TABLE I. Rotational assignment in the 15 V band. The third column has been constructed by taking (P–R difference) $= 2B''(2J'+1)$ and $B'' = 0.11 \pm 0.01$ cm^{-1}. In the fourth column we have taken account of the fact that the absence of nuclear spin implies that J'' must be odd.

Line	P–R difference (cm^{-1})	Calculated J'	Assignment
A	6.99 $\pm$ 0.20	15.4 $\pm$ 1.9	$P(16)$ or $P(18)$
1	3.08 $\pm$ 0.20	6.5 $\pm$ 1.0	$P(8)$
6	1.44 $\pm$ 0.16	2.8 $\pm$ 0.6	$R(2)$
8	2.27 $\pm$ 0.24	4.7 $\pm$ 0.9	$R(4)$
9	3.29 $\pm$ 0.22	7.0 $\pm$ 1.1	$R(6)$

TABLE II. Lines taken from the excitation spectrum in the 15 V band compared with the results of Ochi *et al.* who use a supersonic jet. In the third column # indicates a low intensity line present in the spectrum of Ochi *et al.* (Fig. 2 of Ref. 9) but not shown in Table I of the same publication.

This work		Ochi *et al.*[a]		
ν_{obs} (cm^{-1})	Assignment	ν_{obs} (cm^{-1})	Line	Assignment
31 340.90(A)	$P(16)$ or $P(18)$			
31 343.59		31 343.54	1	
31 343.77				
31 344.03		31 344.03	2	$P(6)$
31 344.25		31 344.24	3	$P(4)$
31 344.37				
31 344.52		31 344.50	4	$P(2)$
31 344.82		#		
31 345.01				
31 345.16		31 345.15	5	$R(0)$
31 345.30(B)		#		
31 345.47				
31 345.65		#		
31 345.77	$R(2)$	31 345.78	6	$R(2)$
31 345.91		31 345.92	7	
31 346.23		#		
31 346.45	$R(4)$	31 346.45	8	$R(4)$
31 346.59		#		
31 346.87	$R(6)$	31 346.86	9	

[a] Reference 9.

TABLE III. Lines taken from the excitation spectrum in the 10 V band compared with the results of Ochi *et al.* (Ref. 9) using a supersonic jet. In the second column # indicates a low intensity line present in the spectrum of Ochi *et al.* but not shown in Table I of the same publication.

This work	Ochi *et al.*[a]		
ν_{obs} (cm^{-1})	ν_{obs} (cm^{-1})	Line	Assignment
30 899.15			
30 899.29			
30 899.43			
	30 899.74	1	$P(8)$
30 899.87	30 899.86	2	$P(4)$
30 899.99	30 899.97	3	$P(6)$
30 900.11	30 900.13	4	$P(2)$
30 900.28	30 900.26	5	$P(4)$
30 900.42			
30 900.56			
30 900.69	#		
30 900.81	30 900.80	6	$R(0)$
30 900.94	#		
30 901.13	#		
30 901.28			
30 901.38	30 901.39	7	$R(2)$
30 901.45			
30 901.62			
30 901.79	30 901.80	8	$R(2)$
30 901.96	#		
30 902.11	#		
30 902.28			
30 902.39	30 902.39	9	$R(4)$
30 902.53			
30 902.64			
30 902.75	#		
30 902.88			
30 903.03	30 903.03	10	$R(6)$
30 903.18			
	30 903.24	11	
30 903.32			

[a] Reference 9.

frequencies still being in quite close agreement. The result is given in Table III. The hot bands represent two-thirds of the intense lines observed in these spectra, and we cannot exclude the possibility that some of them obscure the transitions reported by Ochi. The doublets observed by excitation on the line marked X on the spectrum possess a gap of 8.99 ± 0.52 cm^{-1} which corresponds to a J' of 19.9 ± 3.0. This line must probably be assigned to a $P(20)$ or $P(22)$ transition. The rotational identifications have been arrived at with the aid of a low resolution monochromator (Jobin Yvon HR1000). However, the uncertainties in the value of J' result from the uncertainty in the rotational constant and from the structure of the emission lines.

IV. DISPERSED FLUORESCENCE SPECTRA FROM THE 10 V AND 15 V BAND

In the 15 V band we have excited the transition at 31 346.45 cm^{-1} [$R(4)$], which is the most isolated of the lines marked on the spectrum. For the 10 V band we preferred to be further removed from the crowd of lines positioned between lines 1 and 11 so we excited the transition at 30 899.29 cm^{-1}, marked X on the spectrum [$P(20)$ or $P(22)$]. The dispersed fluorescence spectra for CS_2 have been recorded between 324 and 750 nm for excitation in the 15 V band and between 340 and 700 nm for excitation in the 10 V band. This corresponds, for the 15 V band, to vibrational energies in the ground electronic state between 460 and 18 120 cm^{-1}. After linking up the 125 Å windows, the continuous background was subtracted from the spectrum and finally the abscissae were converted to wave number and the intensities corrected for the response of the OMA. The result for excitation in the 15 V band is given in Fig. 6. In this spectrum we can discern a much greater number of lines than in that obtained from excitation in the 10 V band. The extension of the Franck–Condon access into the red is due to the geometry difference between the ground (linear molecule) and excited (bent molecule) electronic states. The first part of this spectrum ($< 12\,000$ cm^{-1}) is correctly described by an integrable Fermi resonance effective Hamiltonian except near some particular resonances as we will see below. The second part is more complex. Statistical tests we have performed have shown that the low energy spectrum exhibits no spectral correlation in contrast to the behavior the high energy spectrum does. The goal of this paper is to discuss only the first part of the spectrum in order to give a good basis for higher energy study.

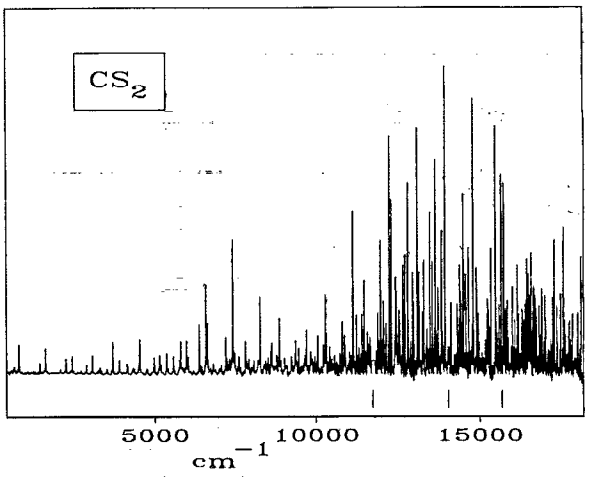

FIG. 6. Resolved fluorescence spectra of CS_2 excited at 31 346.45 cm^{-1} (15 V band). The energies are calculated from the zero point level of the well of the ground electronic state. The dashes beneath the spectrum mark the positions of the lasers lines at 511, 578, and 640 nm, the intensities of which saturates. The intensities of the lines above 16 500 cm^{-1} must be viewed with some caution since the sensitivity of the diode array in this region is less than 5% of its maximum value at 8000 cm^{-1}.

One can consider the rotational quantum number to be sufficiently small that we can neglect rotation. Then the effective Hamiltonian for a linear triatomic molecule is generally taken to be of the form[28]

$$H_0 = \left\langle v_1, v_2^l, v_3 \left| \frac{H}{hc} \right| v_1, v_2^l, v_3 \right\rangle$$

$$= \sum_i \omega_i \left(v_i + \frac{d_i}{2} \right) + \sum_i \sum_{j>i} x_{ij} \left(v_i + \frac{d_i}{2} \right) \left(v_j + \frac{d_j}{2} \right)$$

$$+ y_{222} (v_2 + 1)^3 + g_{22} l^2,$$

where $d_1 = d_3 = 1$, $d_2 = 2$, and

$$g_{22} = \frac{k_{122}^2}{6}\left[-\frac{1}{\omega_1} + \frac{1}{2(\omega_1 + 2\omega_2)}\right] - \frac{x_{22}}{3} - B.$$

This Hamiltonian gives a generally good description of numerous molecules at low energy.

The problem becomes more complicated when there are Fermi resonances present. It is well known that, from an energy of a few thousand cm^{-1}, the vibrational levels of CS_2 are arranged in polyads. The states $|v_1,v_2^l,v_3\rangle$ and $|v_1-1,v_2+2^l,v_3\rangle$ of the polyad, defined by $N = v_1 + v_2/2$ are coupled by a 1:2 Fermi resonance between the ω_1 symmetric stretching mode at 672 cm^{-1} and the ω_2 bending mode at 398 cm^{-1}. The gap $2\omega_2 - \omega_1 = 124$ cm^{-1} is not very small, but the coupling elements are of the same order of magnitude: 30 cm^{-1} at 700 cm^{-1}, 300 cm^{-1} at 12 000 cm^{-1}. In CS_2 the 1:2 Fermi resonance is so strong (the matrix element is of the order of the polyad width) that the normal modes description is therefore no longer valid and the quantum numbers v_1 and v_2 are no longer good quantum numbers. On the other hand, the number N of the polyad remains a good quantum number.[20] It is usual to write the intra polyad coupling between the states $|v_1,v_2^l,v_3\rangle$ and $|v_1-1,v_2+2^l,v_3\rangle$ in the form

$$H_F = \left\langle v_1,v_2^l,v_3\left|\frac{H}{hc}\right|v_1-1,v_2+2^l,v_3\right\rangle$$
$$= \tfrac{1}{2}[v_1(v_2+2+l)(v_2+2-l)]^{0.5}$$
$$\times\left[-\frac{k_{122}}{\sqrt{2}} + \lambda_1 v_1 + \lambda_2(v_2+2) + \lambda_3\left(v_3+\frac{1}{2}\right)\right].$$

The λ_i's are defined in Ref. 13.

A particular coupling between adjacent polyads could be easily described in the effective Hamiltonian by a matrix element which couples the states $|v_1,v_2^l,v_3\rangle$ and $|v_1+2,v_2-2^l,v_3\rangle$ ($\Delta N = \pm 1$)

$$H_c = \left\langle v_1,v_2^l,v_3\left|\frac{H}{hc}\right|v_1-2,v_2+2^l,v_3\right\rangle$$
$$= -\tfrac{1}{2}k_{1122}[v_1(v_1-1)(v_2+2+l)$$
$$\times(v_2+2-l)]^{1/2}.$$

The number of the polyad N is then no longer a good quantum number. We point out finally that if we limit the Hamiltonian to $H_0 + H_F$, then v_3 and N are good quantum numbers and the corresponding actions are constants of motion. This kind of Hamiltonian for a molecule of 3 degrees of freedom is therefore integrable. On the other hand, H_c renders the Hamiltonian nonintegrable and could be one of the origins of chaos.

The fit of the experimental spectra described above shows an agreement with vibron theory and with perturbation theory. We start from a situation in which we consider coupled anharmonic oscillators, and then gradually add perturbations between states where resonances are most likely. In Ref. 20 we show that it is possible to define new variables which allow a correspondence to be made more easily between this effective Hamiltonian and its semiclassical analog and which describe the "more integrable" basis. This is an indispensible requirement if we wish to understand the physical origin of the appearance of vibrational chaos, since we believe that statistical methods do not allow us to explain or even observe the onset of the transition to chaos in molecules.[20]

As N and v_3 are good quantum numbers, of $H_O + H_F$, in Table IV (which gives the results of the fit) and in Figs. 7 and 8 we thus label a line by v_3, by its polyad number N, and by its rank in the polyad, M: M is equal to 1 for the highest level in the polyad and goes to $N+1$ (or $N+1/2$ if v_2 is odd) for the lowest energy level. In the absence of Fermi coupling the terms $M = 1$ correspond to a pure bending vibration and $M = N+1$ to a pure symmetric stretching vibration ($M \equiv v_1 + 1$). The vibrational state $|N, M, v_3\rangle$ in this description corresponds to the state $|v_1 = M-1, v_2 = 2(N+1-M), v_3\rangle$ in the normal mode description.

Bernath's set of parameters[13] is good since it gives a root mean square difference between observed and calculated frequencies of 0.295 cm^{-1}. However, we observe a systematic error which increases as the energy increases [cf. Fig. 9(a)]. As it is possible to linearize the effective Hamiltonian with respect to the parameters, we wrote in Turbo Pascal a program using an algebraic gradient method, which should be able to fit any triatomic molecule spectrum.

First attempts showed that the introduction of one or more of the parameters λ_i caused the system to diverge. Scrutiny of the correlation matrix showed that this was due to the fact that the λ_i are well correlated with the x_{ij}. The parameters λ_i have therefore been held fixed at the values of Bernath *et al.*[13] and the fit performed on the other 11 parameters. The system converges after a few iterations to a set of parameters close to that of Bernath (cf. Table V) with a root mean square difference of 0.21 cm^{-1}. The systematic error has disappeared [cf. Fig. 9(b)] and the only nondiagonal element of the correlation matrix which is greater than 0.9 is that linking x_{22} to y_{222} (-0.985). The standard errors of the parameters are all less than 5% (0.1% for the ω_i) except for the error on y_{222} which is 15%. Table IV gives the observed and calculated lines using the fitted parameters.

The λ_i parameters appear in the H_F as corrections of k_{122} which vary linearly with v_i. The corresponding coupling elements are of the order of 0.5 cm^{-1} at 700 cm^{-1} and 60 cm^{-1} at 12 000 cm^{-1}, which is approximately 1% and 20% of the k_{122} coupling elements. In order to test the significance of the parameters λ_i we have performed a second fit, this time fixing these parameters to 0. Starting with a root mean square difference of 6.41 cm^{-1}, the system reconverges to a root mean square difference of 0.242 cm^{-1}, only 15% greater than that obtained when the three parameters λ_i were nonzero. As we can see in Table V the set of parameters is different this time from that of Bernath, particularly for the parameters x_{11}, x_{12}, and x_{22}. Yet there is no systematic error [cf. Fig. 9(c)], and the only significant element of the correlation matrix is that linking x_{12} to k_{122} (0.993). The uncertainty in the parameters is admittedly greater (27% for x_{12}, 22% for x_{11} and 1% for ω_1), but that is not enough to justify the introduction of these parameters, which are not significant for the large energy domain and the moderate precision with which we are working. These three parameters are nevertheless indispensible if we wish to reproduce

TABLE IV. Overview table of the dispersed fluorescence spectra. (a) Energy calculated from the bottom of the well and adjusted to $J'' = 0$ by the formula: $\nu_{obs} = 31\,346.45 - \nu_{fluo} - 11B$. This formula takes account of the fact that we measure the center of gravity of an unresolved P–R doublet from the spectrum, and that, according to the parameters of Bernath *et al.*, the rotational constant varies by less than 10% between 0 and 12 000 cm^{-1} (we take $B = 0.1091$ cm^{-1}). (b) Energy calculated from the bottom of the well and adjusted to $J'' = 0$ by the formula: $\nu_{obs} = 30\,899.29 - \nu_{fluo(R)}$, where $\nu_{fluo(R)}$ indicates the frequency of the R component of the P–R fluorescence doublet already resolved at 2000 cm^{-1}. (c) An intensity of 100 is assigned to the line at 13 984 cm^{-1} which is the most intense between 0 and 18 000 cm^{-1}. (d) $N = v_1 + v_2/2$ is the number of the polyad, M the order number within the polyad (in the absence of Fermi resonance $M = v_1 + 1$). For even v_2, $l = 0$; for odd v_2, $l = 1$.

ν_{obs} 15 V (cm^{-1}) (a)	ν_{obs} 10 V (cm^{-1}) (b)	Intensity 15 V (c)	Assignment (d)			ν_{obs} 15 V (cm^{-1}) (a)	ν_{obs} 10 V (cm^{-1}) (b)	Intensity 15 V (c)	Assignment (d)		
			N	M	v_3				N	M	v_3
658		2	1	2	0	8 071		4	8,5	3	1
806		10	1	1	0	8 195	8 194	4	10	2	0
1 448		4	2	2	0	8 224		4	12	9	0
1 622		9	2	1	0	8 261		17	11	5	0
2 088	2 088	2	3	3	0	8 326		2	8,5	2	1
2 255		5	3	2	0	8 409		3	12	8	0
2 451	2 451	6	3	1	0	8 436		5	9,5	5	1
2 618		1	4	5	0	8 489	8 487	3	10	1	0
2 723		1	1,5	1	1	8 514	8 513	5	11	4	0
2 891	2 888	3	4	3	0	8 598		7	8,5	1	1
3 077	3 078	6	4	2	0	8 630		10	12	7	0
3 264		1	5	6	0	8 665		2	9,5	4	1
3 287		1	4	1	0	8 784		6	11	3	0
3 354		1	2,5	2	1	8 833		4	13	10	0
3 522		1	5	4	0	8 859	8 858	14	12	6	0
3 534		1	2,5	1	1	8 913		4	9,5	3	1
3 704	3 704	5	5	3	0	9 024		5	13	9	0
3 912		4	5	2	0	9 070	9 067	2	11	2	0
4 142	4 138	2	5	1	0	9 109	9 107	3	12	5	0
4 158		2	3,5	2	1	9 232	9 230	6	13	8	0
4 328	4 328	2	6	4	0	9 259		5	10,5	5	1
4 360		2	3,5	1	1	9 365	9 368	5	11	1	0
4 530		11	6	3	0	9 370	9 370	5	12	4	0
4 754	4 752	2	6	2	0	9 451	9 451	3	13	7	0
4 782		2	4,5	3	1	9 460		7	9,5	1	1
4 974		6	4,5	2	1	9 500		2	10,5	4	1
4 998	4 997	3	6	1	0	9 630	9 629	3	14	10	0
5 149	5 146	6	7	4	0	9 650	9 651	5	12	3	0
5 192		3	4,5	1	1	9 675		4	9	4	2
5 366		7	7	3	0	9 700	9 701	11	13	6	0
5 413		2	8	7	0	9 833		6	14	9	0
5 574	5 578	6	8	6	0	9 911		2	14	3	2
5 603	5 604	2	7	2	0	9 945	9 945	2	12	2	0
5 765	5 764	5	8	5	0	9 960	9 959	6	13	5	0
5 800		10	5,5	2	1	10 037		4	10,5	2	1
5 859		2	7	1	0	10 053	10 052	6	14	8	0
5 977	5 978	10	8	4	0	10 057	10 056	6	15	12	0
6 034		6	5,5	1	1	10 090		2	11,5	5	1
6 198		1	9	7	0	10 168		2	9	2	2
6 210	6 210	1	8	3	0	10 231		8	15	11	0
6 381		15	9	6	0	10 235	10 241	8	13	4	0
6 405		2	6,5	3	1	10 258		4	12	1	0
6 461	6 461	2	8	2	0	10 269		5	10	5	2
6 588	6 587	25	9	5	0	10 292	10 293	11	14	7	0
6 635		15	6,5	2	1	10 328		12	10,5	1	1
6 733	6 731	2	8	1	0	10 342		7	11,5	4	1
6 815	6 815	3	9	4	0	10 433	10 433	7	15	10	0
6 882		2	6,5	1	1				9	1	2
6 997		2	10	7	0	10 494		5	10	4	2
7 061	7 063	3	9	3	0	10 522	10 522	2	13	3	0
7 199		12	10	6	0	10 547		3	14	6	0
7 236		6	7,5	3	1	10 579		6	7,5	1	3
7 324		5	9	2	0				12	13	2
7 421	7 421	42	10	5	0	10 640		3	15	9	0
7 478		7	7,5	2	1	10 676		2	12,5	6	1
7 609	7 606	6	11	8	0	10 743		5	10	3	2
			9	1	0	10 814	10 814	14	14	5	0
7 661	7 662	2	10	4	0	10 828		6	13	2	0
7 809		10	11	7	0	10 836		2	16	12	0
7 919	7 919	5	10	3	0	10 850		2	11	6	2
8 025	8 024	2	11	6	0	10 886	10 885	11	15	8	0

TABLE IV. (*Continued.*)

ν_{obs} 15 V (cm^{-1}) (a)	ν_{obs} 10 V (cm^{-1}) (b)	Intensity 15 V (c)	Assignment (d) N	M	v_3
10 899		6	11,5	2	1
11 010		3	10	2	2
11 035		6	16	11	0
11 077		6	11	5	2
11 136	11 136	25	15	7	0
11 151		27	13	1	0
11 248	11 249	15	16	10	0
11 275		4	17	14	0
11 320		6	11	4	2
11 393	11 393	6	15	6	0
11 414		14	8,5	1	3
			14	3	0
11 437		2	17	13	0
11 479	11 478	21	16	9	0
			12,5	3	1
11 582		14	11	3	2
11 635		10	17	12	0
11 660		11	12	6	2
11 676	11 677	9	15	5	0
11 716		5	14	2	0
11 725		5	16	8	0
11 839		4	17	11	0
11 846		8	14,5	8	1
11 855		7	11	2	2
11 898		15	12	5	2
11 968		10	15	4	0
11 981		43	19	2	3
11 985	11 987	35	32	7	0

the infrared frequencies with precision. The choice of the set of parameters (column 2 or 3 of Table V) therefore depends on the fact that we wish to retain the link with the calculations in the infrared. Finally, we prefer the set ii of Table V because the ω_1 value is closer to the one determined from the high precision ir spectra (column 2).

The effective Hamiltonian adjusted in relation to $H_0 + H_F$ reproduces the experimental spectra well up to 12 000 cm^{-1}. Beyond that, other couplings such as that described in Ref. 20 may be involved. This question will concern us in another paper. Table VI (which will be used below) reports some eigenvectors projected on the normal mode basis $|v_1, v_2\rangle$ ($v_3 = 0$) for the levels $|N = 12, M = 4\rangle$, $|N = 11, M = 1\rangle$, $|N = 11, M = 9\rangle$, and $|N = 10, M = 5\rangle$. Roughly, the wave packets of levels corresponding to a small value of M are mostly centered on the bending motion, while

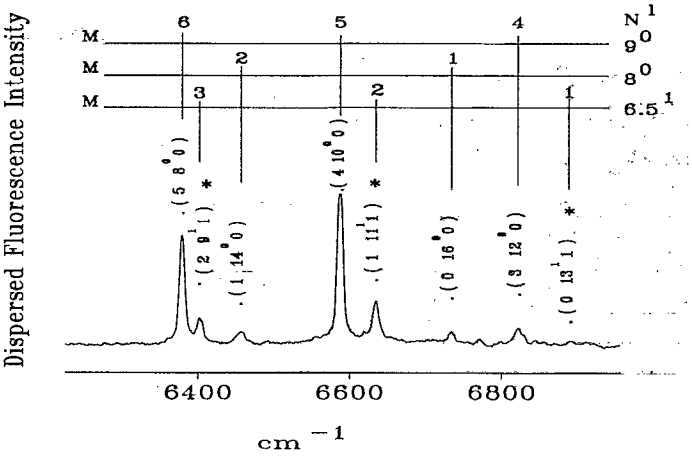

FIG. 8. Resolved fluorescence spectrum of CS_2 excited at 31 346.45 cm^{-1} (15 V band) between 6300 and 6900 cm^{-1}. Above the spectrum we have indicated the assignments of the lines for $v_3 = 0$ and $v_3 = 1$ using the notation $N = v_1 + v_2/2$ and M ($\equiv v_1 + 1$). We also give the normal mode assignment (v_1, v_2^l, v_3) in parenthesis. The stars identify the antisymmetric lines.

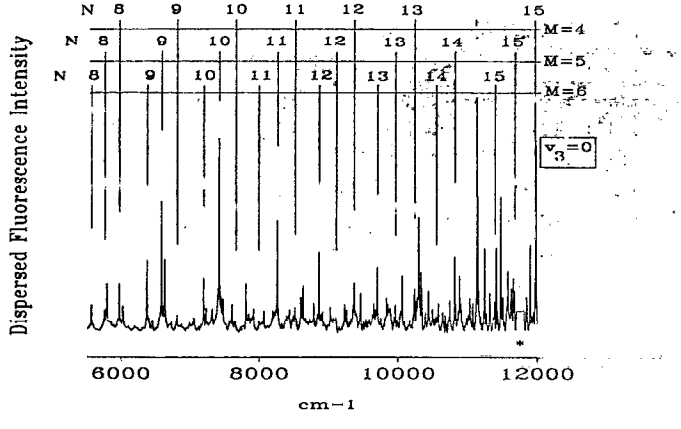

FIG. 7. Resolved fluorescence spectrum of CS_2 excited at 31 346.45 cm^{-1} (15 V band) between 5500 and 12 000 cm^{-1}. Above the spectrum we have indicated the progressions of N for $v_3 = 0$ and $M = 4$, 5, and 6. The star below the spectrum indicates the position of the laser line at 511 nm.

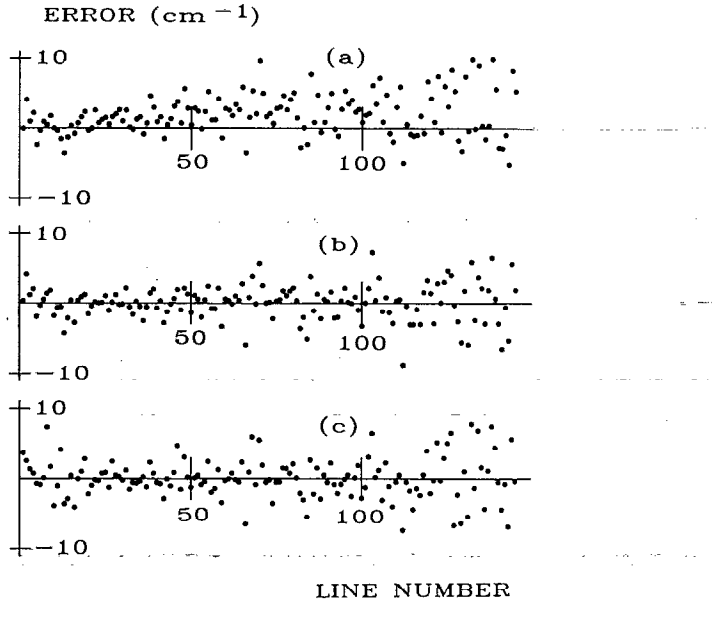

FIG. 9. Differences in cm^{-1} between observed and calculated frequencies for (a) Bernath's parameters (Ref. 13), column 1 of Table V (b) parameters refined with the λ_i fixed at Bernath's values, column 2 of Table V (c) parameters refined with the λ_i set to zero, column 3 of Table V.

TABLE V. Set of parameters (i) of Bernath (ii) adjusted with respect to the results in Table IV by fixing the λ_i to Bernath's values (Ref. 13). (iii) Adjusted with respect to the results in Table IV by fixing the λ_i to zero.

Parameter (cm^{-1})	Bernath[a] (i)	Fixed λ_i (ii)	$\lambda_i = 0$ (iii)
ω_1	672.713	672.562 ± 0.682	665.699 ± 0.641
ω_2	398.135	398.001 ± 0.391	399.835 ± 0.493
ω_3	1558.680	1561.486 ± 1.649	1561.347 ± 1.944
x_{11}	−1.031	−0.990 ± 0.022	−0.175 ± 0.038
x_{12}	−3.152	−3.135 ± 0.028	−1.243 ± 0.332
x_{13}	−7.650	−8.421 ± 0.180	−8.003 ± 0.240
x_{22}	1.210	1.252 ± 0.052	0.770 ± 0.107
x_{23}	−6.446	−6.395 ± 0.101	−6.710 ± 0.140
x_{33}	−6.536	−6.944 ± 0.409	−6.333 ± 0.472
y_{222}	−0.0058	−0.0072 ± 0.0011	−0.0124 ± 0.0012
k_{122}	41.470	41.270 ± 0.832	40.908 ± 1.956
λ_1	0.491	0.491	0.0
λ_2	0.459	0.459	0.0
λ_3	−0.050	−0.050	0.0
rms error (cm^{-1})	0.295	0.210	0.242

[a] Reference 13.

those corresponding to the larger values of M are mostly centered on the symmetric stretching motion. The 1:2 Fermi resonance perturbation is maximum for intermediate M valves; the associated wave packets are more delocalized. In any case, it is clear that the normal mode basis could no longer describe the CS_2 vibrations.

TABLE VI. Eigenvectors of levels $|10, 5\rangle$, $|11, 9\rangle$, $|11, 1\rangle$ and $|12, 4\rangle$ $|N, M\rangle$ in the normal mode basis $|v_1, v_2\rangle$. The levels involved above are either localized on the bending or stretching motion, or completely delocalized. We see that, even at low energy, the normal mode basis is not a good basis for CS_2.

$\|N, M\rangle$	$\|v_1, v_2\rangle$	$C_{v_1 v_2}$	$\|N, M\rangle$	$\|v_1, v_2\rangle$	$C_{v_1 v_2}$
	0,20	0.0394		0,22	0.0003
	1,18	0.1827		1,20	0.0026
	2,16	0.4375		2,18	0.0140
	3,14	0.4719		3,16	0.0547
	4,12	−0.1191		4,14	0.1577
$\|10, 5\rangle$	5,10	−0.4757	$\|11, 9\rangle$	5,12	0.3310
	6,8	0.4934		6,10	0.4622
	7,6	−0.2475		7,8	0.2905
	8,4	0.0749		8,6	−0.2570
	9,2	−0.0135		9,4	−0.4657
	10,0	0.0012		10,2	0.5067
				11,0	−0.1576
	0,22	0.7769		0,24	0.1173
	1,20	−0.5580		1,22	0.3943
	2,18	0.2712		2,20	0.5175
	3,16	−0.1020		3,18	−0.0745
	4,14	0.0312		4,16	−0.4696
$\|11, 1\rangle$	5,12	−0.0079	$\|12, 4\rangle$	5,14	0.4936
	6,10	0.0016		6,12	−0.2823
	7,8	−0.0003		7,10	0.1113
	8,6	0.0000		8,8	−0.0323
	9,4	−0.0000		9,6	0.0070
	10,2	0.0000		10,4	−0.0011
	11,0	−0.0000		11,2	0.0001
				12,0	−0.0000

TABLE VII. Differences, as a function of possible assignments of the parity of v_2 and the value of v_3, between the observed and calculated frequencies for the nine most intense lines of frequency less than 10 000 cm^{-1} that are not well fitted by even v_2 and $v_3 = 0$. For assignments and intensities, refer to Table IV. For even v_2 the calculations have been carried out with $l = 0$, and for odd v_2 with $l = 1$.

ν_{obs} (cm^{-1})	Even v_2 $v_3 = 0$	Odd v_2 $v_3 = 0$	Even v_2 $v_3 = 1$	Even v_2 $v_3 = 2$	Odd v_2 $v_3 = 1$
4974	21	28	−34	−3	−2
5800	−28	0	−2	−65	−2
6635	−28	1	27	−19	−1
7236	−52	0	19	−27	−1
7478	44	−11	−14	−18	1
8071	19	−14	−39	14	−1
8598	64	−20	−23	−60	3
8913	−48	10	45	−21	−1
9259	−26	−14	17	1	−1

Up until now the analysis of fluorescence spectra had highlighted only parallel transitions ($K' - l = 0$) terminating on levels with $v_3 = 0$. If we take the set of parameters fitted by Bernath, all the observed levels up to 12 000 cm^{-1} in the fluorescence spectrum excited via the 10 V band coincide to within ± 6 cm^{-1} of a level calculated with even v_2 and $v_3 = 0$. In contrast, 24 of the 94 lines observed up to 10 000 cm^{-1} in the spectrum excited in 15 V show a much greater difference with the nearest calculated line, the difference sometimes being greater than 60 cm^{-1}. Kasahara *et al.*[10] have not mentioned this fact in their paper concerning a supersonic jet experiment, but if we look carefully at Figs. 4 and 6 of their paper we can make the same conclusion. We have been unable to produce any significant reduction in these differences by refining the set of parameters. The introduction of new parameters in the effective Hamiltonian, some coupling levels within the polyads, others between different polyads, has also met with no success. The supersonic jet experiment cited above and the high intensity of some of these additional lines excludes the possibility of hot bands. We must conclude either that these lines are displaced by perturbations of a greater order or that they must be attributed to levels of odd v_2 and/or nonzero v_3.

We have tested this latter hypothesis on the nine strongest lines that suffer from this problem. The result is given in Table VII. It becomes clear from this that considering these lines as odd v_2 ($l = 1$) to the other lines. We can then proceed and attempt to assign the lines up to 12 000 cm^{-1}. Between 10 000 and 12 000 cm^{-1} there again remain about 12 lines which do not fit well with the levels calculated using the hypotheses (even v_2 and $v_3 = 0$) or (odd v_2 and $v_3 = 1$). Table VIII shows that this time it is necessary to introduce levels with even v_2 and $v_3 = 2$. The set of lines up to 12 000 cm^{-1} is then correctly reproduced by calculation.

However, the introduction of the levels with $v_3 = 1$ and $v_3 = 2$ has multiplied the number of calculated lines by a factor of almost 3, and, the higher we go in energy, the more there is a tendency for there to be two or three calculated lines in order to explain each observed line. Even taking into

TABLE VIII. Differences, as a function of possible assignments of the parity of v_2 and the value of v_3, between the observed and calculated frequencies for the seven most intense lines between 10 000 and 12 000 cm^{-1} which are not well fitted by (even v_2 and $v_3 = 0$) or (odd v_2 and $v_3 = 1$). For the energies and intensities, refer to Table IV. For even v_2 the calculations have been carried out with $l = 0$, and for odd v_2 with $l = 1$.

ν_{obs} (cm^{-1})	Even v_2 $v_3 = 0$	Odd v_2 $v_3 = 0$	Even v_2 $v_3 = 1$	Even v_2 $v_3 = 2$	Odd v_2 $v_3 = 1$
10 269	− 34	− 9	5	6	40
10 494	− 19	− 11	16	− 1	28
10 579	− 66	− 47	7	10	− 56
10 743	− 67	− 6	− 22	− 1	− 60
11 320	> 100	24	17	− 2	29
11 582	− 44	− 13	− 12	0	− 45
11 660	34	7	− 16	0	34

account the fact that the Franck–Condon factor favors the bending modes (where the order number M is small) it becomes difficult to tell which of the calculated lines is correct. We have therefore restricted the assignment to below 12 000 cm^{-1} at which energy the risk of error is still small. In order to go further, it would be necessary to have spectra of greater resolution and greater frequency precision. Nevertheless, this observation is important since the comparison of the spectra arising from the 15 V and the 10 V bands allows us to confirm that the antisymmetric stretching mode does not couple to other modes until 12 000 cm^{-1}. It is also a powerful tool to measure at which energy this coupling will occur. We have shown in Ref. 20 that the vibrational couplings can then be studied quantum mechanically and semiclassically in a subspace of two degrees of freedom and that a pure vibrational chaotic situation can occur at a given energy, since the symmetric stretching vibration and bending vibration belong to the same symmetry.

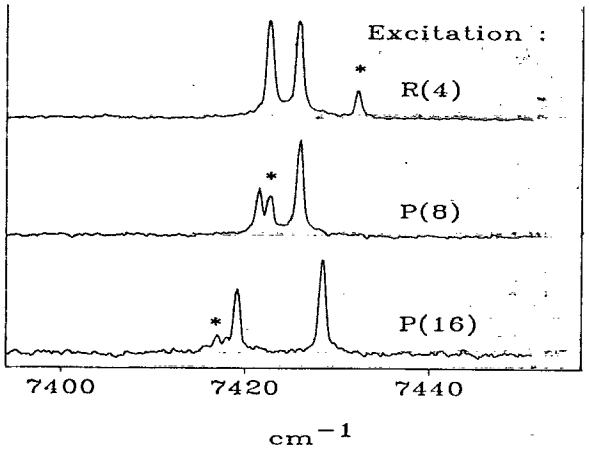

FIG. 10. Observation of a strong perturbation of the emission P–R doublet at 7430 cm^{-1} above the ground state of CS_2. The excitation lines are the $R(4)$ $P(8)$ and $P(16)$ of the 15 V band. Note an extra line (marked by a star) which position changes when J increases. In this example, there is only one extra line because the coupling matrix element is too weak to give enough intensity to the second line of the doublet.

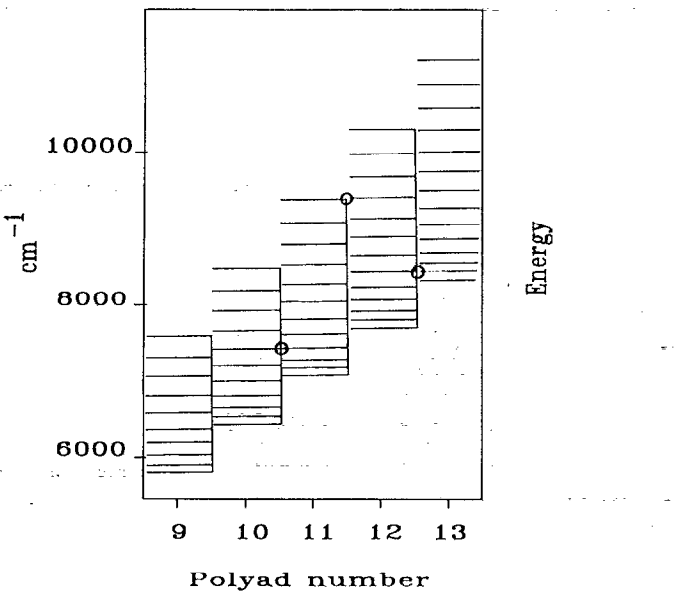

FIG. 11. $N = 9$ to 13 polyads progression calculated with the parameters of Table V. We note three interpolyad crossings with the energy differences: ΔE ($|10,5\rangle$, $|11,9\rangle \cong 1$ cm^{-1}, ΔE ($|11,1\rangle$, $|12,4\rangle \cong 14$ cm^{-1}, ΔE ($|12,8\rangle$, $|13,13\rangle \cong 2$ cm^{-1} (in the $|N,M\rangle$ notation).

Our dispersed fluorescence spectra reveals also that few P–R doublets are strongly perturbed. For example, Fig. 10 shows up a triplet rather than a doublet structure at 7421 cm^{-1}. This transition should connect the $|N = 10, M = 5\rangle$ ($\equiv v_1 = 4$, and $v_2 = 12$) vibrational level of the ground electronic state. It is clear on Fig. 10, that, when the rotational quantum number J' increases, an extra line crosses the P–R doublet and that the intensity of the perturbation is not very sensitive with J'.

V. DISCUSSION

In this section we discuss new experimental results that we have observed in the dispersed fluorescence of CS_2.

A. Inter polyad resonances

There are several vibrational perturbations between 6500 and 9500 cm^{-1} above the ground state. For example, we have observed a strong P–R perturbation at 7430 cm^{-1} (Fig. 10) and a weaker perturbation at 9400 cm^{-1}. Using the polyad labels described above ($N = v_1 + v_2/2$ and M which is equal to $v_1 + 1$ in the absence of Fermi perturbation) these two energies should correspond to the levels $|N = 10, M = 5\rangle$ ($\equiv |v_1 = 4, v_2 = 12\rangle$) and $|N = 11, M = 1\rangle$ ($\equiv |v_1 = 0, v_2 = 22\rangle$). The perturbation at 9400 cm^{-1} has already been observed[29] in a SEP spectrum. Using the set of our fitted vibrational parameters (Table V), the overlaps of polyads 9 through 13 is represented on Fig. 11. This figure clearly shows crossings between the adjacent polyad levels $|10,5\rangle$ and $|11,9\rangle$ at 7430 cm^{-1} and $|11,1\rangle$ and $|12,4\rangle$ at 9400 cm^{-1}. We believe that other resonances than the 1:2 Fermi resonance are responsible for the local perturbations observed. Coriolis couplings could also produce an

TABLE IX. Symmetry (a,b,c), bottom well position (d), bending barrier light (e), bending angle of the equilibrium position (f), and electronic interaction with the $V\,^1B_2$ state (g) of the two lowest energy electronic configurations $(\Pi_g)^4$ and $(\Pi_g)^3\Pi_u$. The $\tilde{X}$, R, S, T, and V labeled states have been experimentally observed. * None observed; ** $A = 88\ cm^{-1}$ (from Ref. 3).

Electronic configuration	(a) $D_{\infty h}$(M) linear	(b) C_{2v}(M) case b	(c) C_{2v}(M) case c	(d) T_{000} (cm^{-1})	(e) Bending barrier (cm^{-1})	(f) Bending angle (°)	(g) Interaction with $V\,^1B_2$
	$^1\Sigma^+$	$^1B_2$	B_2	n.o.*			
	$^1\Sigma_u^-$	$^1A_2$	A_2	32 000[a]		180[a]	
	$^3\Sigma_u^-$	$^3A_2$	A_1, B_1, B_2	n.o.* above V[b]			
$(\Pi_g)^3\Pi_u$	$^1\Delta_u$	$^1B_2(V)$	B_2	30 300 ± 400[c]	1000[c]	150[c]	
		$^1A_2(T)$	A_2	29 430[b,c]	2800[b]	135[b]	$H_{RT} = 2A\Lambda K$ **
	$^3\Delta_u$	$^3B_2(S)$	A_1, A_2, B_1	see Ref. 3			
		$^3A_2(R)$	$A_1, B_1,$	above R			$H_{SJ} \alpha BJ$[c]
			$B_2(R)$	29 300[b]	3000[b]	135[b,d]	$H_{SO} \cong 2A$ **
	$^3\Sigma_u^+$	$^3B_2$	A_1, A_2, B_1	n.o.*			
$(\Pi_g)^4$	$^1\Sigma_g^+(X)$	$^1A_1$	A_1	0		180[c]	

[a] Reference 10.
[b] Reference 3.
[c] Reference 9.
[d] Reference 2.
[e] Reference 1.

anticrossing between these levels but we observed strong perturbations even for small values of J. So, we believe that pure vibrational interactions act first, which is consistent with the fact that CS_2 is a very anharmonic molecule ($k_{122} \sim 40\ cm^{-1}$). As an example the Hamiltonian term H_C (see above) couples adjacent polyads. It has been shown[20] that H_C leads to a chaotic situation because it destroys the polyad quantum number N. Using the creation and annihilation operators (symmetric stretching: a_1, a_1^+; bending: a_2, a_2^+) the third and forth order interactions which mix adjacent polyads are of three types: (i) with no change in bending quantum number: $a_1\ a_2\ a_2^+$ and $a_1\ a_1^+\ a_1$; (ii) with no change in stretching quantum number: $a_1\ a_1^+\ a_2\ a_2$ and $a_2\ a_2\ a_2\ a_2^+$; (iii) with change in both bending and stretching quantum number: $a_1\ a_1\ a_2^+\ a_2^+$ ($\equiv H_C$). The deperturbation process also requires the overlap of the vibrational wave functions of the interacting levels. They are listed on Table VI which shows that the levels involved above are either localized on the bending or stretching motion, or completely delocalized. The difficulty of finding a consistent solution increases drastically as the vibrational energy increases, because the number of anticrossings increases rapidly. A systematic study of such anticrossings using a high resolution spectrum up to 19 000 cm^{-1} is in progress. Nevertheless, we believe that inter polyad anticrossings are the key point for the detailed study of the transition to vibrational chaos.

B. Breaking of the symmetric–antisymmetric selection rule in the excited 15 V band

In contrast with the $2\nu_4 \sim 2\nu_5$ Darling–Dennison resonance in the ground $\tilde{X}$ state of C_2H_2 (Ref. 30), the existence of $v_3 \neq 0$ transitions obviously implies a perturbation in the excited electronic state, because there are not observed when the 10 V band is excited. The excited electronic surface potential of CS_2 along the bending coordinate is rather complicated. In Table IX and Fig. 12 we try to clarify the situation according to the best experimental results and *ab initio* calculations of the literature. The first excited states belong to the configuration $1\ \Pi_u^4\ 1\ \Pi_g^3\ 2\ \Pi_u^1$. This configuration gives 6 electronic states in the linear symmetry, 8 in Hund's case b

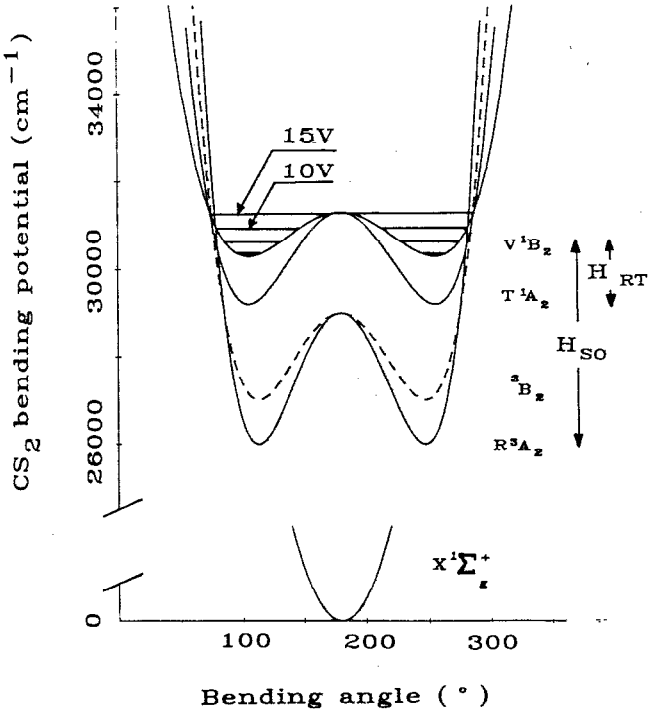

FIG. 12. $V\,^1B_2$, $T\,^1A_2$, $R\,^3A_2$, $S\,^3B_2$, and $X\,\Sigma_g^+$ electronic potentials along the bending coordinate. See Table IX for the barrier and angle parameters.

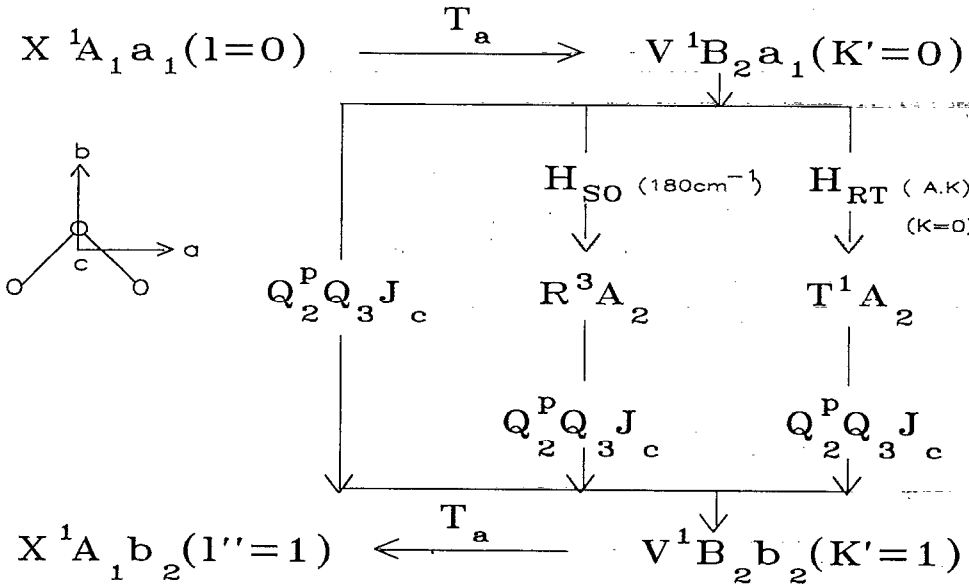

FIG. 13. Possible mechanisms for the breaking of the symmetric–antisymmetric selection rule in the 15 V band of the $V\,^1B_2$ excited electronic state. The $\upsilon_3 \neq 0$ observed dispersed fluorescence lines are interpreted to be due to the $Q_2^3\, Q_3\, J_c$ interaction which is totally symmetric and which couples the bending (0,3,0) and stretching (0,0,1) levels.

of the bent symmetry, and 16 (including spin components) in Hund's case c. Below 31 000 cm^{-1} only three historically named R, T, V states have been observed to date (Fig. 12). The linear singlet $^1\Delta_u$ state is split into two components which have been observed and identified[3] as $^1B_2$ (V) and $^1A_2$ (T) states. The V state, which lies above the T state, is the only state optically allowed by transition from the ground Σ_g^+ ($\tilde{X}$) state. The T state borrows intensity from V through a Renner–Teller interaction which is linear with K. The third observed state is the $^3A_2$ (R) triplet, which is one of the two Renner–Teller components of the linear $^3\Delta_u$ state; the R state borrows intensity from V through a strong spin–orbit interaction (180 cm^{-1}).[3] It is thought that the second component $^3B_2$ is the S absorption system observed by Jungen *et al.*[3] *Ab initio* calculations show that all other states are above 31 000 cm^{-1} except the $^3B_2$ state which correlates with the linear $^3\Sigma_u^+$ state. This state is expected to be between the ground $\tilde{X}\,\Sigma_g^+$ state and the $R\,^3A_2$ state, but has never been observed. In Fig. 12 we report only the states which are observed because of strong coupling to the $V\,^1B_2$ state.

Figure 13 summarizes the possible coupling mechanisms which involve the states R, T, and V and which can explain the breaking of the symmetric–antisymmetric selection rule. In the experimental results we report in this paper, a vibronic $V\,^1B_2\, a_1$ ($K'=0$) state is excited from the ground vibronic $\tilde{X}\,^1A_1\, a_1$ ($l=0$) state (we use the C_{2v} notation, capital letters for the electronic symmetry and small letters for vibrational symmetry). The dispersed fluorescence spectra show transitions from $V\,^1B_2\, b_2$ ($K'=1$) states to $\tilde{X}\,^1A_1$ b_2 ($l''=1$) states. Three interactions, allowed by symmetry, can couple the two $V\,^1B_2\, a_1$ ($K'=0$) and $V\,^1B_2\, b_2$ ($K'=1$) vibronic states. They are

(i) a direct first order Coriolis interaction $Q_2^p\, Q_3\, J_c$ (p is an integer);

(ii) a second order spin–orbit–Coriolis interaction with the intermediate R state;

(iii) a second order Renner–Teller–Coriolis interaction with the intermediate T state.

J_c corresponds to the rotation about the c axis.

The last mechanism is highly improbable because the Renner–Teller interaction is proportional to K which is zero in the present experiment. All of these processes involve the same Coriolis interaction $Q_2^p\, Q_3\, J_c$. A key point is now the vibrational identification of the 10 V and 15 V bands. In 1973 Jungen *et al.*,[3] using a room temperature experiment, gave the following identification for the 10 V and 15 V bands, respectively: (0,0,0) ← (0,0,0) and (0,1,0) ← (0,0,0) (in the normal mode notation); in 1984, Kasahara *et al.*[10] using a supersonic jet experiment, gave, respectively (0,1,0) ← (0,0,0) and (0,2,0) ← (0,0,0); in 1987, Ochi *et al.*[9] in a super cold jet experiment, gave (0,2,0) ← (0,0,0) and (0,3,0) ← (0,0,0). We believe the last result because, using a third body (NH_3) Ochi *et al.* achieved a very vibrationally cold jet of CS_2 and solved the problem of hot bands in the absorption spectrum. Moreover, in these conditions the 15 V band is just below and close to the bending potential barrier of the V state (see Fig. 12). Thus we understand why the 15 V is the more intense band: the 15 V band has a large Franck–Condon overlap with the ground state.

If we believe the identification of Ochi *et al.*, then the breaking of the symmetric–antisymmetric selection rule of the 15 V band corresponds to a direct Coriolis interaction between the bending (0,3,0) ($K'=0$) and antisymmetric stretching (0,0,1) ($K'=1$) levels of the V state. This resonance is very probable if one assumes that the antisymmetric

stretching frequency is close to that of the R state ($\nu_3 \cong 940$ cm^{-1} or 1200 cm^{-1}).[2] The conclusion that the $Q_2^3\ Q_3\ J_c$ Coriolis interaction is responsible for the observed $v_3 \neq 0$ transitions, is also supported by the fact that we observed a rapid change with J of the intensities of the corresponding lines.

VI. CONCLUSION

In this work we have made a detailed study of the dispersed fluorescence spectrum of CS_2 between 0 and 12 000 cm^{-1}. We have shown that, in a cell and at room temperature, it is possible to excite individual rovibronic levels of the molecule using a high resolution dye laser pumped by a copper vapor laser. This experimental work shows that the high repetition rate of a copper vapor laser system is well adapted for extensive molecular spectroscopy. The study of the CS_2 vibrational levels between 0 and 12 000 cm^{-1} has allowed us to assign the lines which appear in the spectra, and to bring to light the levels with $v_3 = 1$ or $v_3 = 2$, by excitation in the 15 V band, which have never before been observed. An effective Hamiltonian and its classical equivalent have been fitted in order to reproduce the observed levels, 11 parameters being sufficient to give a root mean square difference of less than 0.3 cm^{-1}. The polyad number remains a good quantum number, as does v_3, so that this Hamiltonian is integrable even though it is not separable. The strong nondiagonal 1:2 Fermi resonance parameter (~ 40 cm^{-1}) makes CS_2 a very anharmonic molecule and the normal mode basis is not usuable even at low energy (see Table VIII). In Ref. 20 we describe the new set of appropriate quantum numbers for CS_2.

In this paper we have shown that, below 12 000 cm^{-1}, local perturbations are due to higher order Fermi resonances, which couple adjacent polyads. The corresponding couplings render the Hamiltonian nonintegrable.[20] The numbers of double (and multiple) resonances increase with the vibrational energy. At higher energy the "bootstrap" method described in Ref. 31 should be useful to fit the CS_2 spectra. Systematic study of these resonances should be an important tool for understanding the transition to chaos in a simple triatomic system. We also have shown that the breaking of the symmetric-antisymmetric selection rule, observed in the dispersed fluorescence spectra from the 15 V excitation, is due to a direct Coriolis interaction between the bending and antisymmetric stretching levels (0,3,0) and (0,0,1) in the upper state. The dispersed fluorescence spectra from excitation of the level (0,4,0) should be an additional proof. Unfortunately, the $V(0,4,0) \leftarrow \tilde{X}(0,0,0)$ transition is too weak due to a poor Franck–Condon overlap (see Fig. 12). A systematic high resolution study of the dispersed fluorescence lines corresponding to $v_3 \neq 0$ is in progress in order to verify their P–Q–R structure. In any case, the comparison of 10 V and 15 V dispersed fluorescence spectra gives a means of studying the behavior of the antisymmetric stretching mode in the ground electronic state (i.e., at which energy this mode will be coupled to the two others?). A high resolution fluorescence spectrum of CS_2 up to 19 000 cm^{-1} will be discussed in a forthcoming paper in connection with the chaotic behavior of CS_2.

ACKNOWLEDGMENTS

This work was supported by Contract No. 900.3/1308V5655 with the French Conseil Régional de la Région Rhône-Alpes and Contract No. SCI-0034-CCD with the European Economic Community. We are indebted to Oxford Lasers and SOPRA for free technical assistance on the copper vapor laser.

[1] R. S. Mulliken, J. Chem. Phys. **3**, 720 (1935). R. S. Mulliken, Can. J. Chem. **36**, 10 (1958).
[2] B. Kleman, Can. J. Phys. **41**, 2034 (1963).
[3] C. Jungen, D. N. Malm, and A. J. Merer, Chem. Phys. Lett. **16**, 302 (1972); Can. J. Phys. **51**, 1471 (1973).
[4] P. Kusch and F. W. Locmis, Phys. Rev. **55**, 850 (1939).
[5] J. W. Mills and R. N. Zare, Chem. Phys. Lett. **5**, 37 (1970).
[6] A. E. Douglas, Can J. Phys. **36**, 147 (1958); A. E. Douglas and E. R. V. Milton, J. Chem. Phys. **41**, 357 (1964).
[7] J. T. Hougen, J. Chem. Phys. **41**, 363 (1964).
[8] G. W. Loge, J. J. Tiee, and F. B. Wampler, J. Chem. Phys. **84**, 3624 (1986).
[9] N. Ochi, H. Watanabe, and S. Tsuchiya, Chem. Phys. **113**, 271 (1987).
[10] H. Kasahara, N. Mikami, M. Ito, S. Iwata, and I. Suzuki, Chem. Phys. **86**, 173 (1984).
[11] S. J. Silvers and M. R. McKeever, Chem. Phys. **18**, 333 (1976).
[12] A. Matsuzaki and S. Nagakura, Bull. Chem. Soc. Jpn. **49**, 359 (1976).
[13] P. F. Bernath, M. Dulick, R. W. Field, and J. L. Hardwick, J. Mol. Spectrosc. **86**, 275 (1981).
[14] R. Vasudev, Chem. Phys. **64**, 167 (1982).
[15] A. Matsuzaki, Y. Nakamura, and T. Itoh, Chem. Phys. Lett. **87**, 389 (1982).
[16] G. Blanquet and C. P. Courtoy, Ann. Soc. Sci. Bruxelles **88**, 233 (1974), and references therein.
[17] I. Suzuki, Bull. Chem. Soc. Jpn. **48**, 1685 (1975).
[18] G. Sitja and J. P. Pique, Twelfth Colloquium on High Resolution Molecular Spectroscopy, Dijon, France, Sept. 91.
[19] J. P. Pique, J. Opt. Soc. Am. B **7**, 1816 (1990).
[20] J. P. Pique, M. Joyeux, J. Manners, and G. Sitja, J. Chem. Phys. **95**, 8744 (1991)
[21] F. J. Olawsky, M. Ziade, G. Sitja, and J. P. Pique, Proceeding of the Second International Conference Laser M2P, Grenoble (France) (July 91), J. Phys. **4**, C7 (1991).
[22] M. Ziade and J. P. Pique (in preparation).
[23] C. Kittrel, E. Abramson, J. L. Kinsey, S. A. Mc Donald, D. E. Reisner, R. W. Field, and D. H. Katayama, J. Chem. Phys. **75**, 2056 (1981).
[24] W. Demtröder, *Laser Spectroscopy*, (Springer Berlin, 1981), p. 508.
[25] J. P. Pique, F. Stoeckel, and A. Campargue, Appl. Opt. **26**, 3103 (1987).
[26] A. V. Durrant, J. Manners, and P. M. Clark (private communication; to be published).
[27] C. Lambert and G. H. Kimbell, Can. J. Chem. **51**, 2601 (1973).
[28] G. Herzberg, *Molecular Spectra and Molecular Structure, III. Electronic Spectra and Electronic Structure of Polyatomic Molecules* (Van Nostrand Reinhold, New York, 1966).
[29] H. T. Liou, P. Dan, H. Yang, and J. Y. Yuh, Chem. Phys. Lett. **176**, 109 (1991).
[30] K. Yamanouchi, N. Ikeda, S. Tsuchiya, D. M. Jonas, J. K. Lundberg, G. W. Adams, and R. W. Field, J. Chem. Phys. **95**, 6330 (1991).
[31] J. M. Standard, E. D. Lynch, and M. E. Kellman, J. Chem. Phys. **93**, 159 (1990).